

A Dynamic FRET Reporter of Gene Expression Improved by Functional Screening

Martina Schifferer and Oliver Griesbeck*

Max-Planck-Institut für Neurobiologie, Am Klopferspitz 18, 82152 Martinsried, Germany

S Supporting Information

ABSTRACT: Here, we describe a reporter system that consists of a FRET biosensor and its corresponding aptamer. The FRET biosensor employs the synthetic aptamer binding peptide Rsg1.2 sandwiched between mutants of the Green Fluorescent Protein and undergoes FRET when binding its corresponding Rev Responsive Element (RRE) RNA aptamer. We developed a novel approach to engineer FRET biosensors by linker extension and screening to improve signal strength of the biosensor which we called VAmPIRE (Viral Aptamer binding Peptide based Indicator for RNA detection). We demonstrate that the system is quantitative, reversible and works with high specificity *in vitro* and *in vivo* in living bacteria and mammalian cells. Thus, VAmPIRE may become valuable for RNA localizations and as a dynamic RNA-based reporter for live cell imaging. Moreover, functional screening of large libraries as demonstrated here may become applicable to optimize some of the many FRET biosensors of cellular signaling.

Gene expression and its dynamics play a crucial role in all living organisms. Highly complex regulatory mechanisms have involved controlling the transcription of sequences of DNA into RNA molecules with various functions. The deregulation of RNA transcription, processing, transport and controlled degradation is also at the core of various human diseases. Gene expression traditionally is studied using reporter genes such as β -galactosidase, luciferase,¹ green fluorescent protein (GFP),² or β -lactamase,³ which typically require translation and in some cases posttranslational maturation of a protein product that is finally detected. Detection of synthesized RNA is however an alternative approach that promises a more directly coupling to the process of transcription. Techniques to visualize and image RNA predominantly focused on providing specific labels to image trafficking and subcellular localization in live cells. The main techniques for live cell RNA labeling are molecular beacons, RNA–fluorophore complexes and fluorescent protein (XFPs) based approaches.^{4–7} Fluorescent protein based techniques have had a great impact on studying RNA localization. Typically, they employ viral RNA binding peptides that are fused to multiple copies of a XFP and can bind specifically and with high affinity to a short RNA aptamer. The target RNA aptamer can be fused as multimeric repeats to an RNA of interest, thus, allowing an accumulation of XFPs on the labeled RNA. The most prominent labeling systems are based on RNA

binding peptides of the phages MS2^{8,9} and phage lambda.¹⁰ As protein fluorescence itself is not indicative of the interaction of the fluorescent protein labeled peptide with the aptamer, these methods need to operate against background fluorescence or rely on subcellular restriction of the fluorescent protein reporter to the cell nucleus. Split GFP reporter approaches are one means to improve this,¹¹ but the technique also retains some background complementation in the absence of aptamer due to intrinsic affinity of the GFP fragments to each other. In addition, once complemented, the XFP remains fluorescent, even if its bound target RNA is subsequently degraded. We reasoned that a fluorescent protein reporter with conditional aptamer dependent fluorescence properties would be useful to indicate dynamic gene expression. Förster resonance energy transfer (FRET) between suitable mutants of XFPs is a sensitive read-out mechanism to monitor conformational changes in proteins and can be easily imaged by ratiometric read-out of fluorescence intensities¹² or of donor fluorescence lifetimes.¹³ Such an approach has been tried before by constructing a FRET sensor employing the Rev peptide, but due to small signal change was not able to detect RNAs expressed in living cells.¹⁴ To identify other suitable viral aptamer binding peptides for FRET monitoring, we screened a collection of arginine rich high affinity RNA binding peptides for aptamer induced FRET change when sandwiched between donor enhanced Cyan Fluorescent Protein (eCFP) and acceptor Yellow Fluorescent Protein (YFP) variant cpCitrine¹⁵ (Supplementary Table 1, Figure 1A). cpCitrine is a circular permutation of the Citrine that enhances FRET change in calcium biosensors¹⁶ and resulted in larger ratio changes than using Citrine in the current sensor. We identified a number of peptides who initiated conformational change after aptamer binding, leading to increased or decreased FRET in fusion proteins (Supplementary Table 1). Largest emission ratio change upon aptamer addition was found for the bovine immunodeficiency virus (BIV) tat peptide tar aptamer pair¹⁷ (30% ratio change) and the synthetic peptide Rsg 1.2 binding to the human immunodeficiency virus (HIV) RRE (Rev Responsive Element) RNA stem loop IIB34^{18,19} (FR-Rsg1.2, 40% ratio change, Supplementary Table 1). The 32 nucleotide RRE aptamer is a natural target for the HIV Rev protein.²⁰ The synthetic 29 amino acid Rsg 1.2 peptide had been engineered for less α -helical content and higher affinity to and specificity for RRE.^{21,22} We chose the sensor FR-Rsg1.2 for preliminary characterization and further engineering. Specificity of FR-

Received: June 8, 2012

Published: September 4, 2012

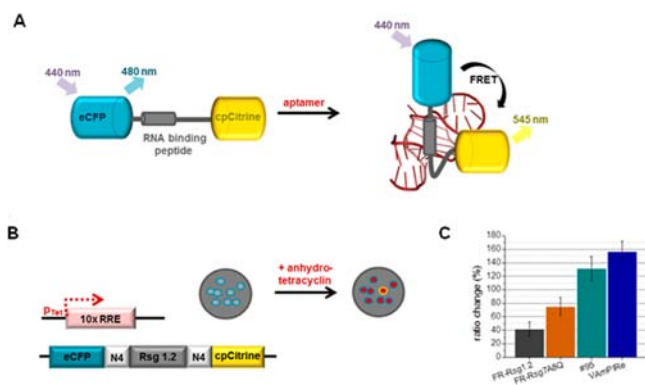


Figure 1. Sensor design and enhancement of FRET change through randomized linker extension. (A) Schematics of sensor design. A collection of arginine rich RNA binding peptides were sandwiched between the fluorescent proteins eCFP and cpCitrine and tested for their ability to initiate conformational change and FRET change when binding their corresponding aptamers. The peptide Rsg 1.2 and the corresponding RRE aptamer were selected for sensor construction. (B) FRET change was enhanced through linker extension and bacterial colony screening. The Rsg1.2 peptide was fused to the donor and acceptor fluorescent proteins via a randomized 4 amino acid linker (N4) on each side. Randomized indicator libraries were co-transformed into bacteria together with a plasmid coding for an inducible 10× concatemer of the RRE aptamer. Functional screening of indicator libraries was performed by widefield CCD camera imaging during induction of 10×RRE aptamer expression (using anhydrotetracycline) (C) Overall aptamer induced FRET ratio change at pH 7.25 in the parental construct (FR-Rsg1.2), the construct with engineered improved physiological pH dependence (FR-Rsg7A8Q) and two indicator variants (#95, #678 or VAmPIRe) picked from the screen.

Rsg1.2 for the RRE aptamer was high compared to the reverse RRE sequence and other aptamers (Supplementary Figure 1). For some RRE single nucleotide mutants with identical secondary structure that have been reported to bind to Rev,²³ a FRET change was observed (Supplementary Figure 1). As signal strength is crucial for use in live cells, we further improved the sensor both by rational design and evolutionary engineering. We noticed that the FRET ratio change was strongly dependent on pH showing higher FRET change at pH values above pH 8. To reduce charge effects, we engineered positively charged residues within the Rsg1.2 peptide in order to shift the performance optimum to a physiological pH (Supplementary Figure 2). Site-specific mutagenesis at the arginine rich N-terminus of Rsg1.2 yielded two mutations (R7A, R8Q) with improved performance at pH 7.25. The combination of these mutations resulted in an overall increase of sensor performance from 40% to 80% change in emission ratio after aptamer binding at physiological pH (Figure 1C, 2b). To further optimize FRET signal strength of the sensor, we devised a method of linker diversification and bacterial colony screening. FRET changes depend on changes in distance and orientation of the donor and acceptor fluorescent protein due to conformational change within the aptamer binding peptide. As these changes are also affected by linking amino acids that orient the fluorophores in free and aptamer-bound state, we designed a library of each 4 random amino acid linkers flanking our optimized Rsg1.2 peptide (Figure 1B, Supplementary Figure 3). The sensor library was cotransformed into bacteria together with a plasmid coding for a tetracycline inducible variant of 10 copies of the RRE aptamer. Using wide field CCD

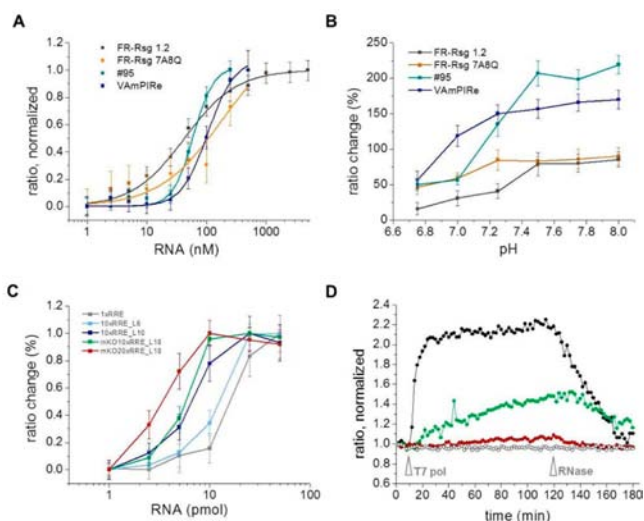


Figure 2. *In vitro* properties of VAmPIRe. (A) Affinity titration of VAmPIRe, mutant #95, FR-RSG7A8Q and the parental FR-Rsg1.2. (B) pH dependence of maximal FRET ratio change in VAmPIRe, #95, FR-RSG7A8Q and FR-RSG1.2. (C) Efficient multimerization and folding of the RRE aptamer. VAmPIRe ratio change at given quantity of RRE aptamer tagged RNA is plotted for an RNA with 1× RRE (gray line), 10× RRE with 6 nucleotide or optimized 10 nucleotide linkers (light blue and dark blue lines), mKO2 ORF tagged 10× RRE and 20× RRE with optimized 10 nucleotide linkers (green and red lines, respectively). (D) Dynamic and reversible imaging of RNA transcription and decay *in vitro*. The T7 promoter (black line and circles) and two less efficient mutant promoters harboring single nucleotide exchanges (blue and red lines and circles) were used for *in vitro* transcription of 10× RRE. Addition of T7 polymerase to start transcription is indicated (T7 pol, arrowhead), as is addition of RNase A (RNase, arrowhead). Note complete reversion of ratio change after degradation of 10× RRE RNA. Transcription of a control RNA not fused to 10× RRE did not elicit any VAmPIRe ratio change (open circles).

camera imaging of bacterial agar plates, we were able to image simultaneously up to 1000 bacterial colonies each harboring a diversified sensor and to follow FRET changes after induction of aptamer expression (Supplementary Figure 4). Overall, about 60 000 indicator variants with diversified linkers were prescreened by imaging and 1500 indicators selected and subsequently purified for further spectroscopic analysis *in vitro*. Linker diversification yielded variants with significantly enhanced FRET change, with the best variants (#678, #95) showing up to 160% maximal change in emission ratio after aptamer binding (Figure 1C, Supplementary Figure 5). This best evolved sensor (#678) was called VAmPIRe (Viral Aptamer binding Peptide based Indicator for RNA detection). VAmPIRe was selected for further *in vitro* characterization (Figure 2). VAmPIRe quantitatively reported aptamer levels (Figure 2A). In analytical size exclusion chromatography, the recombinant purified protein showed a single peak monomeric elution profile (Supplementary Figure 6). Moreover, the sensor allowed dynamic measurements of RNA levels. We set up an *in vitro* transcription reaction including VAmPIRe and three variants of the T7 promoter driving transcription of a construct consisting of 10 copies of the RRE aptamer.²⁴ FRET monitoring allowed to follow differential transcription from these promoters online (Figure 2D). Moreover, subsequent addition of RNase completely abolished FRET changes rapidly (Figure 2D), demonstrating the ability of the sensor to

dynamically and reversibly report RRE aptamer levels in real time *in vitro*. As signal amplification is crucial for successful *in vivo* performance, we tested whether multiple copies of the RRE aptamer could be fused in tandems. We tested variants with 10–30 copies of the RRE aptamer in tandem interspersed with varying numbers of linking nucleotides between them. As simple multiplication of the RRE aptamer was not leading to satisfying results, multimers were initially optimized *in silico* for predicting correct folding of the RRE secondary structure within the multimer repeats using the program mfold²⁵ (Supplementary Figure 7). We then tested these constructs *in vitro* using defined stoichiometric molar ratios of sensor and the corresponding RRE constructs (Figure 2C). These results demonstrated that multimerization resulted in functional concatenated aptamers.

To test the ability of VAmPIRe to report expression of RNA in living cells, we constructed a reporter RNA consisting of the open reading frame (ORF) of the orange fluorescent protein Kusabira Orange 2 (mKO2)²⁶ fused to 20 RRE aptamer repeats. We used ratiometric live cell imaging to follow transcription of mKO2–20×RRE under control of an inducible promoter in HeLa cells. Leakiness of the promoter resulted in minimal mKO2 fluorescence and slightly elevated nuclear VAmPIRe ratios under resting conditions (Figure 3A). Upon induction with tetracycline, RNA levels increased initially within the nucleus. We could then follow mRNA translocation and signal spread from nucleus to the cytosol in real time (Figure 3A,B). Nuclear increases in FRET ratio clearly

preceded increases in cytosolic mKO2 fluorescence by about 1 h. Then, the translation product mKO2 appeared, leading to bright orange fluorescence within cells 6–8 h after induction of expression. Interestingly, RNA levels remained consistently higher in the nucleus than in the cytosol, probably because of incomplete nuclear export. VAmPIRe was an efficient reporter of gene expression. In steady state experiments, cells transfected overnight to express the reporter mKO2 with RRE tag could be easily distinguished by ratiometric imaging from nontransfected cells (Figure 3c). Cells transfected with mKO2 mRNA not fused to RRE exhibited low FRET ratios, demonstrating specificity of RRE tagging (Figure 3D). Addition of the β -actin zipcode mRNA targeting sequence of β -actin²⁷ to mKO2–20×RRE led to significant ratio increases at the leading edges of moving filopodia in transfected migrating NIH mouse fibroblasts (Supplementary Figure 8), showing the potential of VAmPIRe to be used for RNA localization studies within living cells. Methods such as the one developed and used here may become increasingly important in optimizing performance of the many biosensors relying on FRET between fluorescent proteins. Indeed, efforts in this direction have been made in generating small-scale sensor libraries to incorporate combinations of circularly permuted donor and acceptor proteins in a single vector backbone²⁸ or combinations of linkers to optimize FRET.²⁹ Our large-scale screen demonstrated that even relatively short minimal peptide sequences and therefore concomitantly small expected distance changes can be used for sensing in FRET constructs and that FRET in such sensors can be drastically enhanced by linker extension and functional screening.

In conclusion, we provide a dynamic genetically encoded RNA reporter using intramolecular FRET between mutants of GFP. It may be useful in several types of application, for example, as reporter *in vitro* for real time studies on transcription or stability of RNA, to image very dynamic aspects of gene expression *in vivo* or to study relationships between RNA levels and protein expression in single living cells. In particular, studies on RNA localization could profit from the fact that no nuclear restriction of the reporter fluorescent protein is necessary, which may affect proper mRNA localization.⁴ VAmPIRe is potentially targetable to organelles and may enable monitoring import mechanisms, for example, to mitochondria or plastids. It should be pointed out that further improvements are desirable to approach the exquisite signal-to-noise level that, for example, the MS2 system can offer. Such improvements can come from using low level sensor expression systems, brighter and more spectrally separated fluorophores, and further mutagenesis and screening of the sensor and RRE multiaptamers using some of the methods described here.

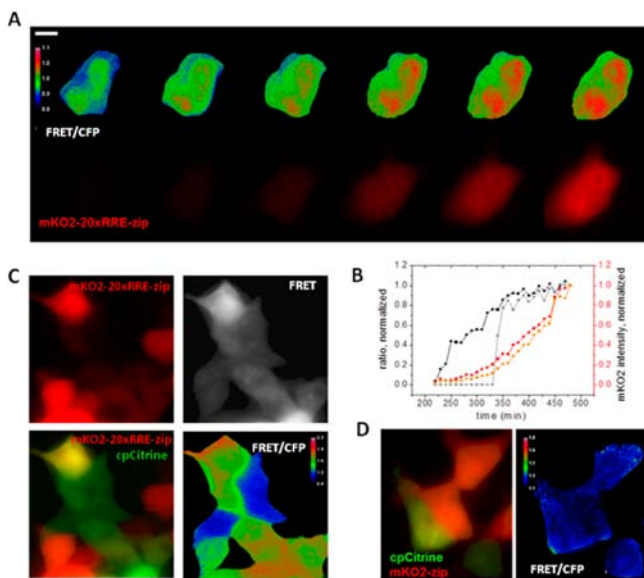


Figure 3. VAmPIRe performance in living mammalian cells. (A) Time course of expression of 20×RRE tagged mRNA coding for mKO2 in a living HeLa cell. Upper lane, VAmPIRe ratio FRET/CFP; lower lane, mKO2 intensity. Scale bar, 20 μ m. (B) Nuclear (black) and cytosolic (gray) ratio and corresponding nuclear (orange) and cytosolic (red) mKO2 intensity plots of the cell depicted in A. (C) VAmPIRe FRET/CFP ratio (right lower image) reports expression of mKO2–20×RRE-zip. A cell that does not express mKO2–20×RRE-zip is distinguished by ratiometric imaging. Right upper image, cpCitrine FRET channel; upper left image, mKO2 intensity channel. Scale bar, 20 μ m. (D) Control HeLa cells expressing VAmPIRe and mKO2-zip mRNA without the RRE tag. Left image, merge of cpCitrine FRET and mKO2 intensity channels; right image, VAmPIRe FRET/CFP emission ratio. Scale bar, 20 μ m.

■ ASSOCIATED CONTENT

Supporting Information

Experimental procedures and supplementary figures 1–8. This material is available free of charge via the Internet at <http://pubs.acs.org>.

■ AUTHOR INFORMATION

Corresponding Author

griesbeck@neuro.mpg.de

Notes

The authors declare no competing financial interest.

■ ACKNOWLEDGMENTS

This work was funded by the Human Frontiers Science Programme (HFSP). We thank Andreas Huettelmaier for the ZBP-mRFP, Atsushi Miyawaki for mKO2, Natalie Broude for the pMB133 constructs, R. Klein for providing cells, A. Geiger and J. Litzlbauer for helpful comments and B. Kunkel and A. Moritz for technical assistance.

■ REFERENCES

- (1) Alam, J.; Cook, J. L. *Anal. Biochem.* **1990**, *188*, 245.
- (2) Tsien, R. Y. *Annu. Rev. Biochem.* **1998**, *67*, 509.
- (3) Zlokarnik, G.; Negulescu, P. A.; Knapp, T. E.; Mere, L.; Burres, N.; Feng, L.; Whitney, M.; Roemer, K.; Tsien, R. Y. *Science* **1998**, *279*, 84.
- (4) Tyagi, S. *Nat. Methods* **2009**, *6*, 331.
- (5) Schifferer, M.; Griesbeck, O. *Integr. Biol.* **2009**, *1*, 499.
- (6) Itzkovitz, S.; van Oudenaarden, A. *Nat. Methods* **2011**, *8*, S12.
- (7) Paige, J. S.; Wu, K. Y.; Jaffrey, S. J. *Science* **2011**, *333*, 642.
- (8) Bertrand, E.; Chartrand, P.; Schaefer, M.; Shenoy, S. M.; Singer, R. H.; Long, R. M. *Mol. Cell* **1998**, *2*, 437.
- (9) Lionnet, T.; Czaplinski, K.; Darzacq, X.; Shav-Tal, Y.; Wells, A. L.; Chao, J. A.; Park, H. Y.; de Turris, V.; Lopez-Jones, M.; Singer, R. H. *Nat. Methods* **2011**, *8*, 165.
- (10) Daigle, N.; Ellenberg, J. *Nat. Methods* **2007**, *4*, 633.
- (11) Valencia-Burton, M.; McCullough, R. M.; Cantor, C. R.; Broude, N. E. *Nat. Methods* **2007**, *4*, 421.
- (12) Miyawaki, A.; Tsien, R. Y. *Methods Enzymol.* **2000**, *327*, 472.
- (13) Levitt, J. A.; Matthews, D. R.; Ameer-Beg, S. M.; Suhling, K. *Curr. Opin. Biotechnol.* **2009**, *20*, 28.
- (14) Endoh, T.; Mie, M.; Kobatake, E. *J. Biotechnol.* **2008**, *133*, 413.
- (15) Griesbeck, O.; Baird, G. S.; Campbell, R. E.; Zacharias, D. A.; Tsien, R. Y. *J. Biol. Chem.* **2001**, *276*, 29188.
- (16) Mank, M.; Reiff, D. F.; Heim, N.; Borst, A.; Griesbeck, O. *Biophys. J.* **2006**, *90*, 1790.
- (17) Chen, L.; Frankel, A. D. *Biochemistry* **1994**, *33*, 2708.
- (18) Malim, M. H.; Tiley, L. S.; McCarn, D. F.; Rusche, J. R.; Hauber, J.; Cullen, B. R. *Cell* **1990**, *60*, 675.
- (19) Daugherty, M. D.; Liu, B.; Frankel, A. D. *Nat. Struct. Mol. Biol.* **2010**, *17*, 1337.
- (20) Battiste, J. L.; Mao, H.; Rao, N. S.; Tan, R.; Muhandiram, D. R.; Kay, L. E.; Frankel, A. D.; Williamson, J. R. *Science* **1996**, *273*, 1547.
- (21) Iwazaki, T.; Li, X.; Harada, K. *RNA* **2005**, *11*, 1364.
- (22) Harada, K.; Martin, S. S.; Tan, R.; Frankel, A. D. *Proc. Natl. Acad. Sci. U.S.A.* **1997**, *94*, 11887.
- (23) Harada, K.; Sugaya, M.; Nishimura, F.; Katoh, A. *Nucleic Acid Symp. Ser.* **2008**, *52*, 13.
- (24) Raskin, C. A.; Diaz, G. A.; McAllister, W. T. *Proc. Natl. Acad. Sci. U.S.A.* **1993**, *90*, 3147.
- (25) Zuker, M. *Nucleic Acids Res.* **2003**, *31*, 3406.
- (26) Sakaue-Sawano, A.; Kurokawa, H.; Morimura, T.; Hanyu, A.; Hama, H.; Osawa, H.; Kashiwagi, S.; Fukami, K.; Miyata, T.; Miyoshi, H.; Imamura, T.; Ogawa, M.; Masai, H.; Miyawaki, A. *Cell* **2008**, *132*, 487.
- (27) Kislauskis, E. H.; Zhu, X.; Singer, R. H. *J. Cell. Biol.* **1994**, *127*, 441.
- (28) Piljic, A.; de Diego, I.; Wilmanns, M.; Schultz, C. *ACS Chem. Biol.* **2011**, *6*, 685.
- (29) Ibraheem, A.; Yap, H.; Ding, Y.; Campbell, R. E. *BMC Biotechnol.* **2011**, *11*, 105.